



Resonance Raman scattering and *ab initio* calculation of electron energy loss spectra of MoS₂ nanosheets



Anirban Chakraborti^a, Arun Singh Patel^{a,*}, Pawan K. Kanaujia^b, Palash Nath^{c,1}, G. Vijaya Prakash^b, Dirtha Sanyal^d

^a School of Computational & Integrative Sciences, Jawaharlal Nehru University, New Delhi 110067, India

^b Nanophotonics Laboratory, Department of Physics, Indian Institute of Technology Delhi, New Delhi 110016, India

^c Department of Physics, University of Calcutta, 92 APC Road, Kolkata 700009, India

^d Variable Energy Cyclotron Centre, 1/AF Bidhannagar, Kolkata 700064, India

ARTICLE INFO

Article history:

Received 26 August 2016
Received in revised form 14 October 2016
Accepted 15 October 2016
Available online 20 October 2016
Communicated by R. Wu

Keywords:

MoS₂
Density functional theory
Electron energy loss
Raman scattering

ABSTRACT

The presence of electron energy loss (EELS) peak is proposed theoretically in molybdenum disulfide (MoS₂) nanosheets. Using density functional theory simulations and calculations, one EELS peak is identified in the visible energy range, for MoS₂ nanosheets with molybdenum vacancy. Experimentally, four different laser sources are used for the Raman scattering study of MoS₂ nanosheets, which show two distinct Raman peaks, one at 385 cm⁻¹ (E_{2g}^1) and the other at 408 cm⁻¹ (A_{1g}). In the cases of three laser sources with wavelengths 405 nm (3.06 eV), 632 nm (1.96 eV) and 785 nm (1.58 eV), respectively, the intensity of E_{2g}^1 Raman peak is more than the A_{1g} Raman peak, while in the case of excitation source of 532 nm (2.33 eV), the intensity profile is reversed and A_{1g} peak is the most intense. Thus a resonance Raman scattering phenomenon is observed for 532 nm laser source.

© 2016 Elsevier B.V. All rights reserved.

1. Introduction

The discovery of graphene in 2004 provided a novel way of studying two dimensional layered structure materials [1–7]. In the recent few years, it has been possible to synthesize different kind of two dimensional nanomaterials of metal chalcogenides, in which d-electrons' interactions can give rise to new physical phenomena. Among these materials, the transition-metal dichalcogenide semiconductor MoS₂ has attracted special attention, as it exhibits intriguing properties [8–13]. Bulk MoS₂ is composed of covalently bonded S–Mo–S sheets that are bound by weak van der Waals forces and is an indirect band gap semiconductor with band gap of the order of 1.2 eV. However, a single layer of MoS₂ is a direct band gap semiconductor with a band gap of 1.9 eV [14,15]. This band gap lies in the visible range and the work function of MoS₂ is compatible with the commonly used electrode materials. Moreover, the single layer of MoS₂ is fluorescent in nature with having quantum yield of the order of 10⁴ more than the bulk MoS₂ [16]. Thus MoS₂ has potential applications in electronic, optoelectronic

and photonic devices [16,2,17]. For example, the field effect transistors based on MoS₂ show high on/off switching ratio [15], which is of the order of 10⁸.

There are numerous studies on the intriguing properties and broad applications of MoS₂ nanosheets; only recently, a study by Bruno et al. reported the resonance Raman scattering in MoS₂ nanosheets [18]. Conventionally, the EELS spectroscopy can be used to find out the band gap in semiconducting materials. It has been studied that the doping in semiconductors causes tuning in the band gap of these materials. In this work, we have studied the effect of different kinds of vacancies (Mo, S) in the EELS spectra of MoS₂ nanosheets, and attempt has been made to correlated theoretical results of EELS with the Raman spectroscopic study. For the first time we have tried to correlate the theoretical results of EELS to the Raman spectroscopic results. It is found that molybdenum vacancy in MoS₂ nanosheets shows a EELS peak around 2.4 eV and Raman spectroscopic study shows enhancement of A_{1g} peak at 532 nm laser excitation source, thus a resonance Raman scattering phenomenon is observed at 2.3 eV excitation source.

2. Methods

2.1. Computational methods

For the theoretical modeling and density functional theory (DFT) calculations, we have used the Vienna Ab Initio Simula-

* Corresponding author.

E-mail addresses: anirban@jnu.ac.in (A. Chakraborti), arunspatel.jnu@gmail.com (A.S. Patel).

¹ Current affiliation: School of Physical Sciences, National Institute of Science Education and Research, HBNI, Jatni – 752050, India.

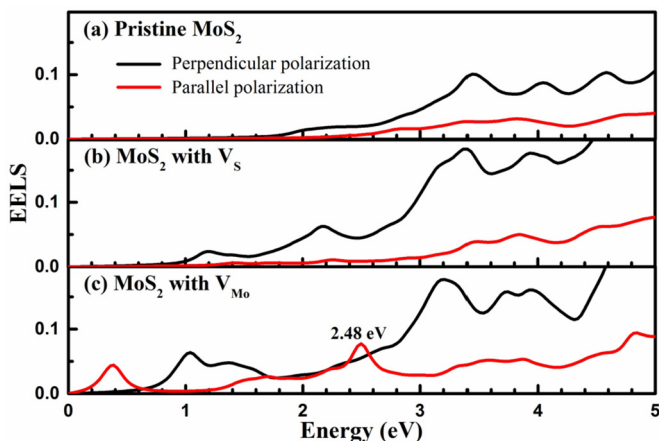


Fig. 1. Electron energy loss spectra of (a) pristine MoS₂ nanosheets, (b) MoS₂ nanosheets with sulfur vacancy (V_S) and (c) MoS₂ nanosheets with molybdenum vacancy (V_{Mo}). The black line denotes perpendicular polarization and the red line denotes parallel polarization. (For interpretation of the references to color in this figure legend, the reader is referred to the web version of this article.)

tion (VASP) code [19–22], along with the MedeA software package. Before the evaluation of frequency dependent dielectric properties, all the structures were geometrically relaxed until the unbalanced force components converge below 0.02 eV/Å. Simulations were performed under the generalized gradient approximation (GGA) with Perdew–Burke–Ernzerhof (PBE) exchange and correlation [23,24]. A mesh cutoff energy of 400 eV, has been set in the expansion of plane wave basis sets and the electronic ground state convergence criterion has been set by 10^{-5} eV for all the systems. The Brillouin zone (BZ) has been sampled by $7 \times 7 \times 1$ Monkhorst–Pack (MP) grid point [25]. Electron energy loss spectra (EELS) of pristine MoS₂ system, MoS₂ system with sulfur vacancy and MoS₂ system with molybdenum vacancy have been explored in the framework of density functional theory (DFT).

2.2. Experimental methods

The proposed theoretical model is supported by Raman spectroscopic study of MoS₂ sheets. The MoS₂ nanosheets were prepared by chemical exfoliation method [26]. For this purpose, 1 g of bulk MoS₂ powder was mixed with 1 mL of N-Methyl-2-pyrrolidone (NMP) and the mixture was ground for 30 min in mortar pestle. The paste like mixture was put in vacuum oven at room temperature over night. The mixture was redispersed into 20 mL of NMP solvent and ultra-sonicated for 10 h using 25 W ultrasonication bath. After ultrasonication, the mixture was centrifuged to separate out the MoS₂ nanosheets. The supernatant was collected from the solution which contained MoS₂ nanosheets. Such obtained dispersion of MoS₂ sheets were drop cast on silicon substrate and annealed above 220 °C for Raman and scanning electron microscopic (SEM) studies. For transmission electron microscopic (TEM) analysis the solution was put on carbon coated copper grid and dried at room temperature.

3. Results and discussion

3.1. DFT calculation

In DFT calculations, first the frequency dependent dielectric function ($\epsilon(\omega)$) of a system has been computed; then electron energy loss spectra (EELS) of this system have been evaluated using the relation: $L(\omega) = \text{Im}(-1/\epsilon(\omega))$. From EELS (see Fig. 1) it is identified that the spectrum shows asymmetrical nature in between two polarization states of electromagnetic (EM) wave;

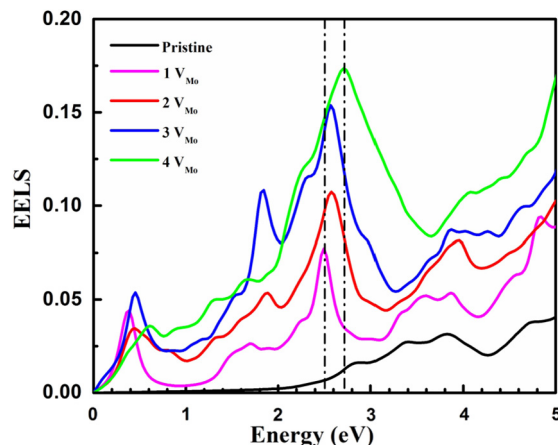


Fig. 2. Electron energy loss spectra of MoS₂ nanosheets with varying concentrations of molybdenum vacancy (V_{Mo}). The black line denotes parallel polarization for pristine MoS₂. A single molybdenum vacancy ($1V_{Mo}$) is depicted by the magenta line; $2V_{Mo}$ by red, $3V_{Mo}$ by blue, and $4V_{Mo}$ by green, respectively. (For interpretation of the references to color in this figure, the reader is referred to the web version of this article.)

which is the manifestation of layered structure of MoS₂. The results for the electronic energy loss spectra for MoS₂ nanosheets are shown in Fig. 1.

Pristine MoS₂ system does not exhibit any significant loss peak in the visible range below 3.0 eV optical frequency. Besides, defect induced systems such as MoS₂ with sulfur vacancy as well as MoS₂ with molybdenum vacancy both demonstrate the existence of low energy loss peak in the visible part. Atomic vacancy induces localization of electron density near the vacancy site that actually gives rise to new plasmon excitations in the visible range as observed from EELS. One of the interesting features observed from EELS is that the emergence of new loss peaks in the infrared to visible part at 0.4 eV and 2.48 eV optical frequency for perpendicular polarization (E_{\perp}) in case of molybdenum vacancy system (see Fig. 1 (c)). Besides, there exists no signature of such loss peaks in case of E_{\perp} polarization in both pristine and sulfur vacancy system.

Since MoS₂ nanosheet is a two dimensional material with a layered structure, the in-plane (X–Y plane) symmetries are different from the out of plane (perpendicular direction) symmetries. Thus, the associated chemical bonding and electron distribution are different along the perpendicular direction compared to the in-plane direction, which results in formation of two different excitation modes in the in-plane direction and perpendicular plane direction of the MoS₂ nanosheet. In general, they occur at different excitation energies also. The presence of V_{Mo} in the structure gives rise to electron localization at the vacancy site, on the MoS₂ layer. These localized electrons result in a distinct, out-of-plane excitation peak (or EELS peak) at ~ 2.5 eV energy. Note that no excitation peak exists at the similar energy in case of in-plane plasma oscillation. To confirm the existence of the EELS peak at ~ 2.5 eV energy, DFT calculations were performed for several systems having various molybdenum vacancies V_{Mo} or defect concentrations. Interestingly, it is noted that the increase of vacancy concentration enhances the EELS peak height (see Fig. 2). Moreover, a little blue shift of the peak position is observed with increasing defect concentration, although the shift does not affect the final results and conclusions of this present observation.

3.2. TEM analysis

Presence of sheets like structure in MoS₂ was confirmed by transmission electron microscope image analysis. The TEM images were obtained by a transmission electron microscope (model

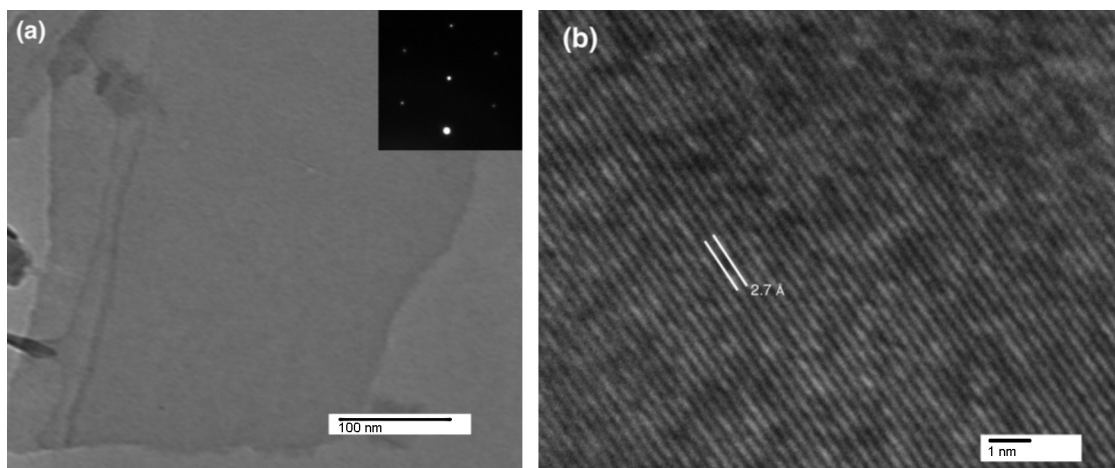


Fig. 3. TEM images of (a) MoS₂ nanosheets, with inset showing SAED pattern (scale equals 100 nm); (b) lattice spacing in MoS₂ nanosheet (scale equals 1 nm).

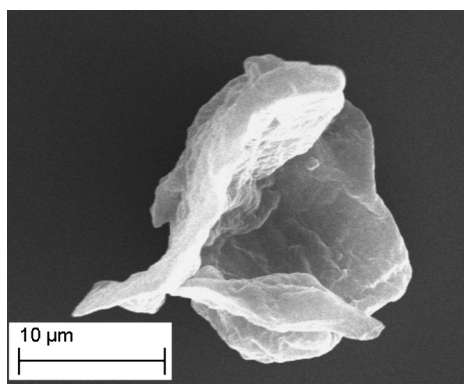


Fig. 4. SEM image of MoS₂ nanosheets.

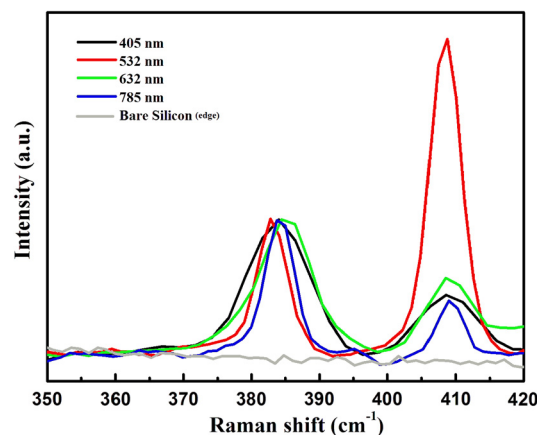


Fig. 5. Raman spectra of MoS₂ nanosheets for different laser excitation sources: 405 nm (3.06 eV), 532 nm (2.33 eV), 632 nm (1.96 eV) and 785 nm (1.58 eV). The Raman spectrum of bare silicon (edge) is plotted in grey. (For interpretation of the references to color in this figure legend, the reader is referred to the web version of this article.)

JEOL-2100F, Japan), operating at 200 kV. The TEM image of MoS₂ nanosheets is shown in Fig. 3.

The inset of Fig. 3(a) shows the selective area electron diffraction (SAED) pattern from MoS₂ nanosheet. Fig. 3(b) shows the lattice spacing in MoS₂ nanosheet. The lattice spacing between adjacent planes is of the order of 2.7 Å which corresponds to (100) plane.

3.3. SEM analysis

The SEM image of MoS₂ nanosheets was recorded by scanning electron microscope (Zeiss EVO40). The sheets like structure of MoS₂ was observed in the scanning electron microscopy. The SEM image of MoS₂ nanosheets is shown in Fig. 4. The size of these nanosheets is of order of 10 μm.

3.4. Raman spectroscopic study

The Raman spectra of MoS₂ were collected by Renishaw inVia confocal Raman spectrometer using four different excitation laser sources 405 nm, 532 nm, 632 nm and 785 nm. For 405 nm and 532 nm lasers the associated grating is 2400 lines per mm while for 632 nm and 785 nm lasers it is 1200 lines per mm. The Raman spectra were collected by using 50X objective lens having numerical aperture 0.25.

Fig. 5 shows the Raman spectra of MoS₂ nanosheets. The spectra consist two Raman peaks one at 385 cm⁻¹ and other at 408 cm⁻¹. The Raman peak at 385 cm⁻¹ is known as E_{2g}¹ peak and other at 408 cm⁻¹ is A_{1g} peak, these peaks originate due to in plane and out of plane vibrations of S–Mo–S bonds. The effect

of excitation source on the Raman peaks of MoS₂ nanosheets has been analyzed. For all three wavelengths of laser sources, 405 nm (3.06 eV), 632 nm (1.96 eV) and 785 nm (1.58 eV) the intensity of E_{2g}¹ peak is greater than the intensity of A_{1g} peak while in case of 532 nm (2.33 eV) excitation source the intensity of A_{1g} is more than that of the E_{2g}¹ peak. Our theoretical analysis shows that an EELS peak is observed around 2.48 eV. Hence the enhancement of the Raman peak is due to the resonance occurring at 532 nm. The Mo vacancy in MoS₂ causes localization of electron density near the vacancy site. This vacancy gives rise to new plasmon excitations (i.e., a new energy level) in the visible range as observed from EELS. Due to the localized electron density, the Raman inelastic scattering cross section of A_{1g} vibrational peak increases. The observation is similar to the surface enhanced Raman scattering, where the enhanced electromagnetic field near metallic surface causes enhancement in the Raman signals of the molecules in the vicinity of metallic surface [27].

In order to verify whether the intensity enhancement of A_{1g} Raman peak under 532 nm laser excitation, comes from the Si/SiO₂ substrate, we tested the Raman response in the bare area of the sample (without the MoS₂) to see Si/SiO₂ substrate. Here, we have used edge Si, since it may have more native SiO₂. As evident from Fig. 5, there is no conflict of SiO₂ Raman peaks within the region of MoS₂ peaks and the intensity enhancement of the A_{1g} peak

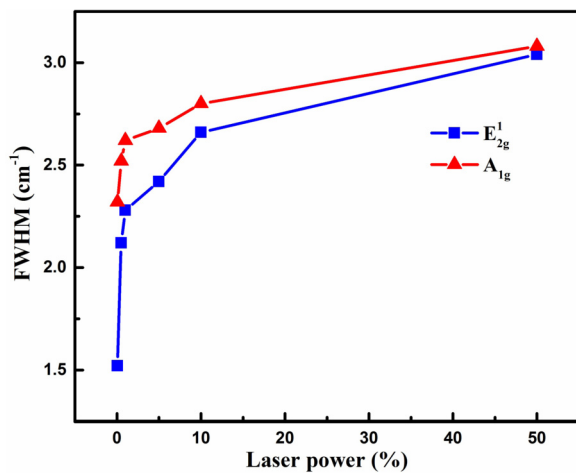


Fig. 6. Effect of laser (532 nm) power on the full width half maximum (FWHM) of E_{2g}^1 and A_{1g} peaks of MoS₂ nanosheets.

(identified at 2.48 eV in the visible range for MoS₂ nanosheet with molybdenum vacancy) comes from a resonance Raman scattering, and certainly not from the Si/SiO₂ substrate.

The effect of laser power on the full width half maximum (FWHM) of both the peaks has been studied using 532 nm laser source (Fig. 6). With increase in the power of laser the FWHM value of E_{2g}^1 and A_{1g} peaks increases and attains a saturation level.

4. Conclusions

In summary, we have demonstrated the presence of EELS peak in molybdenum disulfide (MoS₂) nanosheets in the visible energy range. Theoretically, using DFT simulations and calculations, an EELS peak was identified at 2.48 eV (visible range), for MoS₂ nanosheets with molybdenum vacancy; for pristine MoS₂ and MoS₂ with sulfur vacancy, the EELS did not show any resonance peaks for parallel polarization. This was then confirmed experimentally, using four different laser sources for the Raman scattering study of MoS₂ nanosheets. In the cases of three laser sources with wavelengths 405 nm (3.06 eV), 632 nm (1.96 eV) and 785 nm (1.58 eV), respectively, the intensity of E_{2g}^1 Raman peak was more than the A_{1g} Raman peak, while in the case of excitation source of 532 nm (2.33 eV), the intensity profile was reversed and A_{1g} peak was the most intense. Such a resonance phenomena may trigger some new features such as generation of localized energy states. The presented 2D nanosheets have a great potential for future optical systems, especially in nanophotonic devices operating at visible wavelengths.

Acknowledgements

AC acknowledges the financial support by institutional research funding IUT (IUT39-1) of the Estonian Ministry of Education and Research. AC and ASP acknowledge financial support from grant number BT/BI/03/004/2003(C) of Government of India, Ministry of Science and Technology, Department of Biotechnology, Bioinformatics division. Authors thank the AIRF, JNU for TEM and SEM characterizations and the FIST (DST, Govt. of India) UFO scheme of IIT Delhi for Raman/PL facility.

References

[1] K.S. Novoselov, A.K. Geim, S. Morozov, D. Jiang, Y. Zhang, S. Dubonos, I. Grigorieva, A. Firsov, Electric field effect in atomically thin carbon films, *Science* 306 (5696) (2004) 666–669.

[2] K.F. Mak, C. Lee, J. Hone, J. Shan, T.F. Heinz, Atomically thin MoS₂: a new direct-gap semiconductor, *Phys. Rev. Lett.* 105 (13) (2010) 136805.

[3] B. Radisavljevic, A. Radenovic, J. Brivio, V. Giacometti, A. Kis, Single-layer MoS₂ transistors, *Nat. Nanotechnol.* 6 (3) (2011) 147–150.

[4] J. Kibsgaard, Z. Chen, B.N. Reinecke, T.F. Jaramillo, Engineering the surface structure of MoS₂ to preferentially expose active edge sites for electrocatalysis, *Nat. Mater.* 11 (11) (2012) 963–969.

[5] P. Nath, S. Chowdhury, D. Sanyal, D. Jana, Ab-initio calculation of electronic and optical properties of nitrogen and boron doped graphene nanosheet, *Carbon* 73 (2014) 275–282, <http://dx.doi.org/10.1016/j.carbon.2014.02.064>, <http://www.sciencedirect.com/science/article/pii/S000862231400205X>.

[6] J. Lin, H. Li, H. Zhang, W. Chen, Plasmonic enhancement of photocurrent in MoS₂ field-effect-transistor, *Appl. Phys. Lett.* 102 (20) (2013) 203109.

[7] J. Shakya, A.S. Patel, F. Singh, T. Mohanty, Composition dependent Fermi level shifting of Au decorated MoS₂ nanosheets, *Appl. Phys. Lett.* 108 (1) (2016) 013103.

[8] F. Prins, A.J. Goodman, W.A. Tisdale, Reduced dielectric screening and enhanced energy transfer in single- and few-layer MoS₂, *Nano Lett.* 14 (11) (2014) 6087–6091.

[9] Y. Wang, J.Z. Ou, S. Balendhran, A.F. Chrimes, M. Mortazavi, D.D. Yao, M.R. Field, K. Latham, V. Bansal, J.R. Friend, et al., Electrochemical control of photoluminescence in two-dimensional MoS₂ nanoflakes, *ACS Nano* 7 (11) (2013) 10083–10093.

[10] J.Z. Ou, A.F. Chrimes, Y. Wang, S.-y. Tang, M.S. Strano, K. Kalantar-zadeh, Ion-driven photoluminescence modulation of quasi-two-dimensional MoS₂ nanoflakes for applications in biological systems, *Nano Lett.* 14 (2) (2014) 857–863.

[11] A. Castellanos-Gomez, M. Poot, G.A. Steele, H.S. van der Zant, N. Agrait, G. Rubio-Bollinger, Elastic properties of freely suspended MoS₂ nanosheets, *Adv. Mater.* 24 (6) (2012) 772–775.

[12] J.A. Miwa, S. Ulstrup, S.G. Sorensen, M. Dendzik, A.G. Čabo, M. Bianchi, J.V. Lauritsen, P. Hofmann, Electronic structure of epitaxial single-layer MoS₂, *Phys. Rev. Lett.* 114 (2015) 046802, <http://dx.doi.org/10.1103/PhysRevLett.114.046802>, <http://link.aps.org/doi/10.1103/PhysRevLett.114.046802>.

[13] Y. Zheng, J. Chen, M.-F. Ng, H. Xu, Y.P. Liu, A. Li, S.J. O'Shea, T. Dumitrică, K.P. Loh, Quantum mechanical rippling of a MoS₂ monolayer controlled by inter-layer bilayer coupling, *Phys. Rev. Lett.* 114 (2015) 065501, <http://dx.doi.org/10.1103/PhysRevLett.114.065501>, <http://link.aps.org/doi/10.1103/PhysRevLett.114.065501>.

[14] R. Ganatra, Q. Zhang, Few-layer MoS₂: a promising layered semiconductor, *ACS Nano* 8 (5) (2014) 4074–4099.

[15] T. Sreeprasad, P. Nguyen, N. Kim, V. Berry, Controlled, defect-guided, metal-nanoparticle incorporation onto MoS₂ via chemical and microwave routes: electrical, thermal, and structural properties, *Nano Lett.* 13 (9) (2013) 4434–4441.

[16] A. Splendiani, L. Sun, Y. Zhang, T. Li, J. Kim, C.-Y. Chim, G. Galli, F. Wang, Emerging photoluminescence in monolayer MoS₂, *Nano Lett.* 10 (4) (2010) 1271–1275.

[17] R. Wang, B.A. Ruzicka, N. Kumar, M.Z. Bellus, H.-Y. Chiu, H. Zhao, Ultrafast and spatially resolved studies of charge carriers in atomically thin molybdenum disulfide, *Phys. Rev. B* 86 (2012) 045406, <http://dx.doi.org/10.1103/PhysRevB.86.045406>, <http://link.aps.org/doi/10.1103/PhysRevB.86.045406>.

[18] B.R. Carvalho, L.M. Malard, J.M. Alves, C. Fantini, M.A. Pimenta, Symmetry-dependent exciton-phonon coupling in 2D and bulk MoS₂ observed by resonance Raman scattering, *Phys. Rev. Lett.* 114 (2015) 136403, <http://dx.doi.org/10.1103/PhysRevLett.114.136403>, <http://link.aps.org/doi/10.1103/PhysRevLett.114.136403>.

[19] G. Kresse, J. Hafner, Ab initio molecular dynamics for liquid metals, *Phys. Rev. B* 47 (1) (1993) 558.

[20] G. Kresse, J. Hafner, Ab initio molecular-dynamics simulation of the liquid-metal-amorphous-semiconductor transition in germanium, *Phys. Rev. B* 49 (1994) 14251–14269, <http://dx.doi.org/10.1103/PhysRevB.49.14251>, <http://link.aps.org/doi/10.1103/PhysRevB.49.14251>.

[21] G. Kresse, J. Furthmüller, Efficiency of ab-initio total energy calculations for metals and semiconductors using a plane-wave basis set, *Comput. Mater. Sci.* 6 (1) (1996) 15–50.

[22] G. Kresse, J. Furthmüller, Efficient iterative schemes for ab initio total-energy calculations using a plane-wave basis set, *Phys. Rev. B* 54 (1996) 11169–11186, <http://dx.doi.org/10.1103/PhysRevB.54.11169>, <http://link.aps.org/doi/10.1103/PhysRevB.54.11169>.

[23] J.P. Perdew, K. Burke, M. Ernzerhof, Generalized gradient approximation made simple, *Phys. Rev. Lett.* 77 (1996) 3865–3868, <http://dx.doi.org/10.1103/PhysRevLett.77.3865>, <http://link.aps.org/doi/10.1103/PhysRevLett.77.3865>.

[24] J.P. Perdew, K. Burke, M. Ernzerhof, Generalized gradient approximation made simple [Phys. Rev. Lett. 77, 3865 (1996)], *Phys. Rev. Lett.* 78 (1997) 1396, <http://link.aps.org/doi/10.1103/PhysRevLett.78.1396>.

[25] H.J. Monkhorst, J.D. Pack, Special points for Brillouin-zone integrations, *Phys. Rev. B* 13 (1976) 5188–5192, <http://dx.doi.org/10.1103/PhysRevB.13.5188>, <http://link.aps.org/doi/10.1103/PhysRevB.13.5188>.

- [26] Y. Wang, J.Z. Ou, A. Chrimes, B. Carey, T. Daeneke, M.M.A. Alsaif, M. Mortazavi, S. Zhuiykov, N.V. Medhekar, M. Bhaskaran, et al., Plasmon resonances of highly doped two-dimensional MoS₂, *Nano Lett.* 15 (2) (2015) 883–890.
- [27] B. Sharma, R.R. Frontiera, A.-I. Henry, E. Ringe, R.P. Van Duyne, SERS: materials, applications, and the future, *Mater. Today* 15 (1) (2012) 16–25.